2022 Update for the Differences Between Thermodynamic Temperature and ITS-90 Below 335 K

Christof Gaiser[1], Bernd Fellmuth[1], Roberto Gavioso[2], Murat Kalemci[3], Vladimir Kytin[4], Tohru Nakano[5], Anatolii Pokhodun[6], Patrick M.C. Rourke[7], Richard Rusby[8], Fernando Sparasci[9], Peter Steur[2], Weston Tew[10], Robin Underwood[9], Rod White[11], Inseok Yang[12], Jintao Zhang[13]

[1] Physikalisch-Technische Bundesanstalt (PTB), Abbestrasse 2-12, 10587 Berlin, Germany
[2] Istituto Nazionale di Ricerca Metrologica (INRiM), Strada delle Cacce 91, 10135 Torino, Italy
[3] TÜBİTAK UME (UME) Gebze Yerleşkesi P.K. 54 41470 Gebze/KOCAELİ, Turkey
[4] All-Russian Research Institute of Physical Technical and Radio Technical Measurements (VNIIFTRI) Mendeleevo, Solnechnogorsky District, 141570 Moscow Region, Russia
[5] National Metrology Institute of Japan (NMIJ, AIST) Tsukuba Central 3, 1-1-1 Umezono, Tsukuba, Ibaraki 305-8563 Japan
[6] D. I. Mendeleyev Institute for Metrology (VNIIM), Moskovsky pr., 19, 190005 St. Petersburg, Russia
[7] National Research Council Canada (NRC), 1200 Montreal Road, Ottawa, ON K1A 0R6, Canada
[8] National Physical Laboratory (NPL), Hampton Road, TW11 0LW, Teddington, United Kingdom
[9] Laboratoire Commun de Métrologie (LNE-CNAM), 61 rue du Landy, 93210 La Plaine-Saint-Denis, France
[10] National Institute of Standards and Technology (NIST), 100 Bureau Dr, Gaithersburg, MD 20899, USA
[11] Measurement Standards Laboratory (MSL), 69 Gracefield Road, Lower Hutt 5010, New Zealand
[12] Korea Research Institute of Standards and Science (KRISS), Daejeon 34113, South Korea
[13] National Institute of Metrology (NIM), Beijing 100029, People's Republic of China

Abstract

In 2011, a working group of the Consultative Committee for Thermometry published their best estimates of the differences between the thermodynamic temperature T and its approximation (T_{90}), the temperature according to the International Temperature Scale of 1990, ITS-90. These consensus estimates, in combination with measurements made in accordance with ITS-90, are an important alternative to primary thermometry for those requiring accurate measurements of thermodynamic temperature. Since 2011, there has been a change in the definition of the kelvin and significant improvements in primary thermometry. This paper updates the ($T - T_{90}$) estimates by combining and analysing the data used for the 2011 estimates and data from more recent primary thermometry. The results of the analysis are presented as a 12th-order polynomial representing the updated consensus values for the differences and a 6th-order polynomial for their uncertainty estimates.

Keywords: Thermodynamic temperature, primary thermometry, International Temperature Scale, ITS-90, gas thermometry

1. Introduction

On 20 May 2019, four of the base units of the International System of Units (SI) were redefined by fixing the values of four fundamental physical constants [1] (for details see [2]). Among

these, the base unit of thermodynamic temperature has been defined by fixing the value of the Boltzmann constant, rather than by fixing the temperature of a particular state of matter [3]. The new definition eliminates the uncertainty in the realisation of the triple point of water from the realisation of the kelvin and encourages direct realisation of the kelvin using any thermodynamic method appropriate for the temperature of interest. In the *mise en pratique for the kelvin* (*MeP*-K), the Consultative Committee for Thermometry (CCT) identifies the primary methods that are both well documented and achieve state-of-the-art uncertainties [4, 5]. Primary methods are especially important for scientific purposes.

However, primary methods are not suited to routine thermometry: all require a high level of expertise, and most are very slow and require expensive, often custom-built equipment. Additionally, primary methods have historically had unacceptably high measurement uncertainties [3]. The solution has been for the CIPM to define more practical International Temperature Scales (ITS) approximating thermodynamic temperatures using defined reference temperatures and interpolating thermometers. The International Temperature Scale of 1990, ITS-90 [6], is the current basis for internationally consistent temperature measurements, denoted T_{90}, and defines scale temperatures from 0.65 K up to the highest measurable temperatures. The uncertainty of its realisation ranges from a few tenths of a millikelvin below 335 K and increases to several millikelvin at 1225 K [7]. ITS-90 was defined so that the scale temperatures, T_{90}, corresponded closely to the known thermodynamic temperatures, T, at the time of definition.

As primary methods improve, the differences between T and T_{90} become increasingly apparent. In 2011, CCT Working Group 4 published the then best estimates of the differences ($T - T_{90}$) [8]. This paper is the basis for the CCT guide "*Estimates of the Differences between Thermodynamic Temperature and the ITS-90"* [9]. Use of ITS-90 combined with knowledge of $T–T_{90}$ is an important alternative to primary thermometry.

Since 2011, several primary methods have undergone significant improvements accompanying research undertaken to determine the Boltzmann constant for the redefinition of the kelvin [10, 11]. Subsequently, the improved methods have been used to measure $T–T_{90}$ over temperatures ranging from 4 K to 323 K. The CCT Working Group for Contact Thermometry (CCT-WG-CTh) has now collated the new data and combined them with those published in [8] to update the best estimates of ($T - T_{90}$).

The data used in the analysis are presented in Section 2. Section 3 then identifies a polynomial representation of ($T - T_{90}$) versus T_{90} and summarises the considerations in its

development. Section 4 discusses uncertainties associated with the estimates of (T - T_{90}), and how they are to be applied. Finally, Section 5 summarises the results and conclusions.

2. Overview of literature data

For the 2011 estimates, the input data and the uncertainties were provided by the researchers in polynomial form and evaluated at the temperatures listed in Table 1. Especially in the case of the data published before 1990, corrections were required for the change in scale from IPTS-68 [6], and some uncertainties required harmonisation following the publication of the *Guide to the Expression of Uncertainty* (GUM) [12]. This review was carried out by WG-4 in a process lasting more than 5 years. The corrected and harmonised data in Table 1 constitutes the first part of the input for the present work [1]. It includes data from ten research groups using one of three primary methods:

- Acoustic Gas Thermometry (AGT): INRIM (polynomial based on data from [13]), LNE-NIST (polynomial based on data from [14]), NIST (polynomial based on data from [15-17]), UL-ICL (polynomial based on data from [18]);
- Dielectric-Constant Gas Thermometry (DCGT): PTB (in [8] a polynomial based on data from [19, 20] was used; this data was revised in [21] due to systematic changes in the compressibility values of the capacitors; in Table 1, therefore, the revised values from [21] are listed; in view of the large amount of data points, only 12 from 22 measuring temperatures between 4 K and 25 K given in [21] are used; the interpolation between the points and uncertainties was performed via cubic splines);
- Constant-Volume Gas Thermometry (CVGT): VNIIFTRI (Polynomial based on data from [22]), KOL (Polynomial based on data from [23] recalculated by WG4 at that time to interpolate in ranges with very few data points), NMIJ (Polynomial based on data from [24]), NML (Polynomial based on data from [25]), NPL (Polynomial based on data from [26]).

[1] To reproduce the numbers given in Table 2 of [7], the following information is needed. Between 4.2 K and 24.5 K and from 290 K up to 335 K (and above) simple weighted means of the tabulated values and the associated uncertainties were calculated (for the PTB data, the original data also listed in Table 1 in grey was used). (At 303 K a double counting of one data set in the evaluation of [7] led to a slightly different value (the correct value at 303 K would have been (T-T_{90}) = 4.18 mK with an uncertainty of 0.48 mK).) From 35 K to 70 K the so-called BOB method (the name comes from Type **B O**n **B**ias, see M.S. Levenson *et al.* J. Res. Natl. Inst. Stand. Technol. 105, 571 (2000), section 4) and the associated uncertainty was used. From 77 K to 255 K the weighted mean was calculated, and its uncertainty was multiplied with a factor according to the Student's distribution (k = 2) considering the individual degrees of freedom at the specific temperature.

Table 1

The data measured after 2011 and the related uncertainties are given in Table 2. The new results are from eight research groups using one of four primary methods:

- Acoustic Gas Thermometry (AGT): INRIM (Table 1 in [27]), NIM (Tables 14 and 15 in [28]), NPL (Table 1 in [29]), VNIIFTRI (Abstract in [30]); LNE-TIPC (Table 1 in [31], the values are not explicitly stated but obvious), NMIJ (Table 1 in [32]);
- Dielectric-Constant Gas Thermometry (DCGT): PTB (Table 2 in [21], Table 2 in [33], Table 2 in [34]);
- Refractive-Index Gas Thermometry (RIGT): NRC (Abstract in [35]), INRIM (Table 1 in Corrigendum [36]), TIPC-LNE (Table 9 in Corrigendum [37]);
- Constant-Volume Gas Thermometry (CVGT): NMIJ (Figure 4 in [38], the data in Table 1 of this publication is a private communication).

The previous definition of the kelvin fixed the temperature of the triple point of water (TPW), T_{TPW}, to 273.16 K with zero uncertainty, so that $(T - T_{90})_{\mathrm{TPW}}$ was identically zero. This was reflected in the 2011 estimates in which the least-squares fit and uncertainty were forced to zero at the TPW [8].

On 20 May 2019, the new definition of the kelvin took effect, and the Boltzmann constant was fixed to the final CODATA adjusted value with zero uncertainty [1, 39]. Although T_{TPW} remained 273.16 K at the moment of redefinition, it acquired an uncertainty of 0.1 mK transferred from the Boltzmann constant experiments, and it is no longer fixed. A corresponding data point, $(T - T_{90})_{\mathrm{TPW}} = 0.0(1)$ mK, is included in the fitted data, and the $D(T_{90})$ polynomial fit to the $(T - T_{90})$ data, see next section, has not been forced to zero at the TPW. This reflects the fact that the value of T_{TPW} is no longer defined.

Table 2

3. Fitting-function selection and tests

The aim of the analysis is to develop a smooth analytic function, $D(T_{90})$, describing the best estimate of $T–T_{90}$ as a function of the measured scale temperature, T_{90}. Ideally the function should cover the full range of the data, 4 K to 323 K, and achieve the best compromise between capturing the underlying structure of the data, while not exhibiting excessive sensitivity to measurement errors, i.e., overfitting. In the temperature range of interest, all data (including that used to establish ITS-90) was obtained with various types of gas thermometer for which all the known forms of measurement errors are free of asymptotic or exponential effects that

might cause discontinuities or other difficult-to-fit artefacts in the data. Therefore, there was a reasonable expectation that a fitted function based on a power series with linear coefficients would be both satisfactory and the simplest choice:

$$D(T_{90})/\,\mathrm{mK} = (T - T_{90})/\,\mathrm{mK} = \sum_{i=0}^{n} a_i (T_{90}/\mathrm{K})^i \cdot \qquad (1)$$

It was the consensus of CCT-WG-CTh that all data listed in Table 1 and Table 2 were fitted together. The least-squares software used for the analysis employs Björck's orthonormal modification of the Gram-Schmidt algorithm [40, 41], which minimises the effects of round-off errors in the numerical computations. To confirm the correct operation of the software, the computations were checked using a generalised non-linear least-squares application written by Saunders [42, 43] employing the iterative Levenberg-Marquardt algorithm [44]. Saunders' application was also used to calculate the propagated uncertainties and in numerical experiments evaluating the effects of correlations. An important benefit of the Björck algorithm is that the polynomials are orthonormal in the set of arguments (set of independent variables). The use of orthogonal functions has the advantage that the coefficients are independent of each other. Furthermore, their magnitude allows a rigorous but simple test for the selection of an appropriate fitting order. This selection is an important task since one must avoid either of the extremes of too high an order with a resultant overfit and unrepresentative oscillations or of too low an order with a resultant underfit and loss of experimental information. The left part of Figure 1 shows the natural logarithm of the absolute values of the orthogonal coefficients obtained with the Björck algorithm for data listed in Tables 1 and 2 in dependence on the fitting order. If the fitting functions are necessary for describing the data (called "true or signal functions" in [45]), there is a tendency of decreasing absolute value, i.e., the coefficients converge. But the coefficients of further, not necessary ("noise") functions show no tendency to converge. From Figure 1 it can, therefore, be concluded that the order 11 or 12 may be sufficient.

One further traditional statistical test for the quality of a least-squares fit is the chi-square test. If all the uncertainty estimates, u_i, are correct and the measurement errors are independent and normally distributed, the weighted least-squares sum minimised by the software,

$$\chi^2 = \sum_{i=1}^{N} \frac{\left[(T - T_{90})_i - D(T_{90})\right]^2}{u_i^2}\,, \qquad (2)$$

is a sample drawn from a chi-square distribution with the degree of freedom $\nu = N\text{-}k$, where N is the number of data points and k is the number of coefficients in the fitted function.

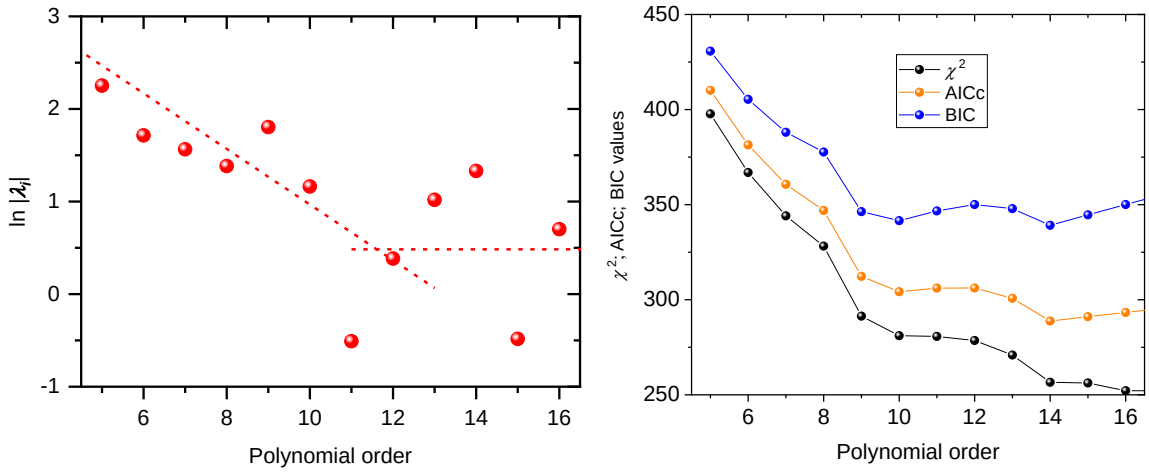

Figure 1: Left: Natural logarithm of the absolute values of the orthogonal coefficients λ_i, obtained by fitting power series to the $(T - T_{90})$ data listed in Tables 1 and 2 applying the Björck algorithm, in dependence on the fitting order. The dashed lines are a line fit to the steep and a fit of a constant to the flat part of the data, respectively. Their intersection suggests a 11th or 12th order fit. Right: Statistical measures for fit quality vs polynomial order: χ^2, AICc, and BIC (for details see text).

Typically, the calculated χ^2 value falls as the order of the fit increases and converges to a constant value when there is no more structure to be detected in the data. If the asymptotic value for χ^2 is too large or too small, then one or more of the assumptions is incorrect. Figure 2 shows that the residuals to the weighted fit are very nearly normally distributed, and the χ^2 value calculated from the fits of order larger than 10 to the combined data of Table 1 and Table 2 is also within expected bounds. While the chi-square test is a useful indicator confirming that a model is consistent with measurement uncertainties, it is not a discerning test of fit order.

Two commonly used tests for the quality of fit are based on the Bayesian Information Criterion (BIC) and the Akaike Information Criterion with the small-number correction (AICc) (for details see [46]). For a weighted least-squares fit using normally distributed data with correctly estimated uncertainties, both the AICc and the BIC for an nth-order polynomial can be expressed as:

$$BIC = k\ln(N) + \chi^2, \tag{3}$$

and

$$AICc = 2k + \frac{2k(k+1)}{N-k-1} + \chi^2, \tag{4}$$

with $k = n+2$.

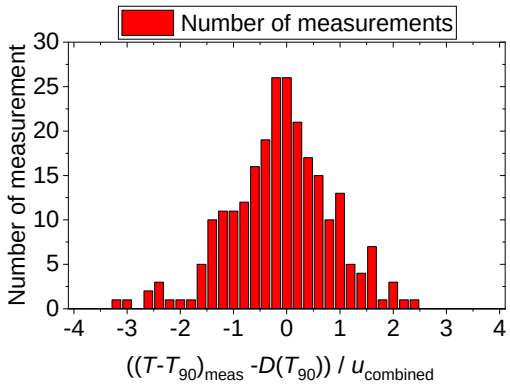

Figure 2: Number of measurements versus the ratio of the deviation between the single experiment $(T\text{-}T_{90})_{\mathrm{meas}}$ and $D(T_{90})$ to the combined uncertainty of the single experiment and $u(D(T_{90}))$, u_{combined}.

The right part of Figure 1 plots the values of χ^2, AICc, and BIC versus the fit order, n. The optimum fit order is identified by the minimum of the curves. There is a subtle difference between the two criteria. Ideally, the minimum of the BIC identifies the model that is the best descriptor of the analysed data, whereas the minimum of the AICc identifies the model that is the best predictor of new data. Since the polynomial is to be used to correct new temperature measurements, the AICc is the appropriate measure of fit quality. It suggests that any polynomial in the range 11th- to 13th-order would be similarly satisfactory. The BIC and AICc tests are comparative measures, but they do not indicate that we have found the best of all possible models. Therefore, there is still a requirement for the model to be reasonable and to fit the data well. In addition to the evidence from the χ^2 value and the distribution of residuals showing that the model is reasonable, a visual inspection of the data and the fitted polynomials showed that there was little difference between all of models of 11th- order and above, except for a small 'bulge' in the residuals near 320 K, which largely disappeared with the 12th-order model.

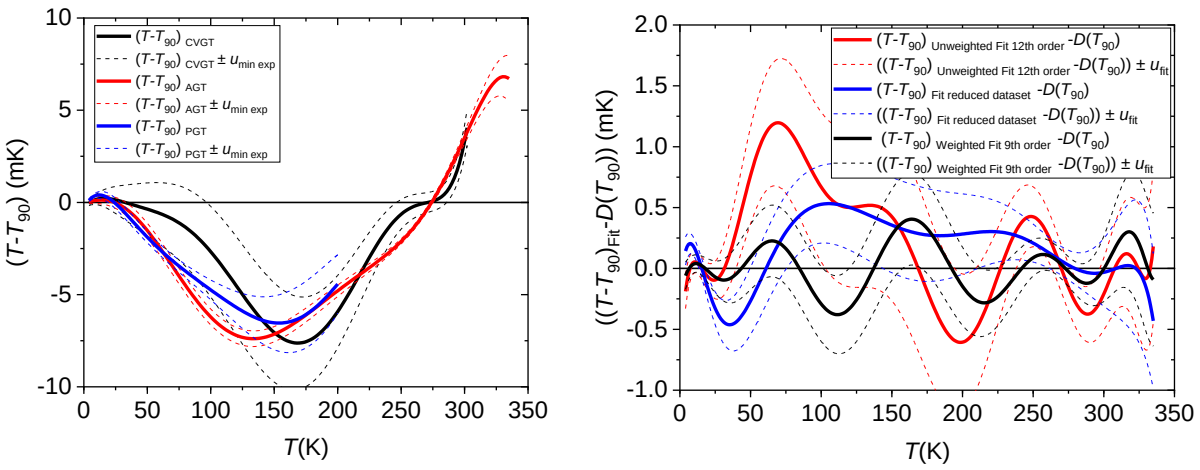

Figure 3: Left: The data listed in Tables 1 and 2 was allocated in data sets for the three primary thermometer types CVGT, AGT and PGT (polarizing gas thermometry, PGT, combines DCGT and RIGT as defined in the *MeP*-K [4, 5]). The results of weighted fits of 7th order of (T-T_{90}) versus temperature for the three primary thermometers are shown as solid lines. The thin dashed lines of specific colour envelop the range (T-T_{90}) ± u_{minexp}, with u_{minexp} corresponding to the minimal single-experiment standard uncertainty estimates and marked in Tables 1 and 2 by asterisk. Right: Deviation of different fitting results from the function $D(T_{90})$ obtained by a weighted 12th order fit: Blue line: reduced dataset (see text); Red line: unweighted 12th order fit of the complete dataset; Black line: weighted 9th order fit. The thin dashed lines of specific colour envelop ((T-T_{90})$_{fit}$-$D(T_{90})$) ± u_{fit}, with the specific standard fitting uncertainty estimates u_{fit}.

To test for some hidden uncertainty components due to the use of different primary thermometers, the data sets listed in Tables 1 and 2 were allocated in three groups. The first one is the CVGT group, the second one the AGT group, and the third one the PGT group, which combines data from both DCGT and RIGT. A separate study of DCGT and RIGT is not reasonable due to similarity of the methods. The only difference is the detection technique, which is in the case of DCGT a capacitance measurement and in the case of RIGT a microwave frequency measurement. Therefore, both techniques have been merged to PGT (see *MeP*-K [4, 5]). The three individual data sets have been treated in the same way as the complete dataset discussed before. The only difference is the use of fit order seven instead of twelve to avoid oscillations. The uncertainty estimates are simply the smallest uncertainties of individual experiments for the specific temperature range (marked with an asterisk in Tables 1 and 2). In the left part of Figure 3 it is clearly shown that all primary thermometers agree well within their

uncertainties. This is a strong argument that the datasets can be treated together as one data set, and a splitting into individual primary thermometers is not necessary.

The following stability checks of the result have been made. The first test was performed with a reduced dataset, where the number of data points was almost halved. In particular, the most accurate data from [29] has been thinned out. The choice was random with the idea to demonstrate that the fit is not solely dominated by the data with the lowest uncertainty. The specific points used for the reduced dataset are marked in red in Table 2. The next check was performed with an unweighted fit of 12th order to the complete dataset, and finally a weighted 9th order fit was made. All deviations relative to the weighted 12th order full-data-set fit $D(T_{90})$ are shown in the right part of Figure 3. It is clearly visible that the fitting result is extremely stable. $D(T_{90})$ is neither dominated by the fit order nor, in most parts, by the weighting of a specific dataset. The reason for the larger deviation of the unweighted fit between 50 K and 100 K is that most of data in this range has larger uncertainties and larger deviations from the overall fit. This has no effect on the weighted fit, but leads to stronger, unrealistic deviations for the unweighted fit. In other temperature ranges, this is not the case.

Finally, the 12th-order polynomial was chosen: the coefficients are given in Table 3, and the agreement between the fit function $D(T_{90})$ and the individual experimental data $(T - T_{90})_{meas}$ is analysed as follows. Figure 2 plots a histogram of the normalised residuals of the fit, $((T - T_{90})_{meas} - D(T_{90})) \ / \ u_{combined}$, where $u_{combined}$ is the combined uncertainty of the fit and the uncertainties listed in Tables 1 and 2. Ideally, the normalised residuals should be normally distributed. The actual distribution is close to normal, perhaps very slightly skewed, and has most of the 219 points within ±3, as expected. There are also no conspicuous outliers. In Figure 4 the experimental data together with $D(T_{90})$ is plotted, and in Figure 5 corresponding residuals are shown with a remarkable consistency between the residuals and the uncertainties. Evidently, the number of outliers is negligible, and their deviations are tolerable.

The fitted polynomial is continuous in all derivatives over the range of the data and has a slope at TPW of 0.132(6) mK K^{-1}. In contrast, the 2011 formulation of $D_{2011}(T_{90})$ used different analytical functions below and above TPW, with slopes of 0.070 mK K^{-1} (below TPW) and 0.101 mK K^{-1} (above TPW) [8]. The steeper slope of the present work reflects the extra detail from new low-uncertainty acoustic gas thermometry measurements in the vicinity of the TPW [27-29]. No anomaly in thermodynamic temperature, T, is expected at TPW, but the scale temperature, T_{90}, has small discontinuities in the first and third derivatives due, respectively, to the different ITS-90 interpolating equations [3,47] and the different reference functions [48] below and above TPW.

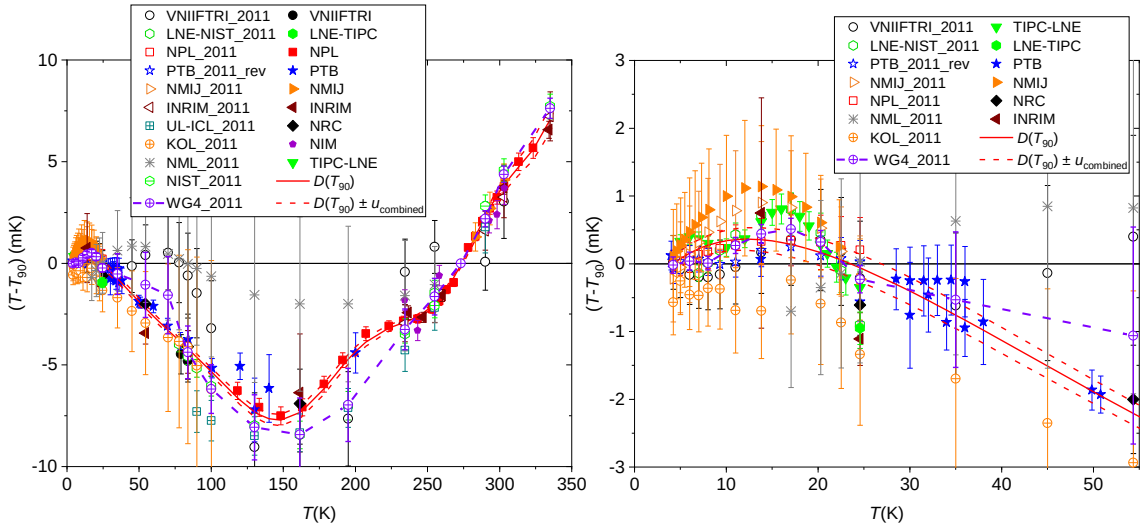

Figure 4: Left: $(T - T_{90})$ data as listed in Tables 1 and 2 versus temperature T_{90}. The institutes at which the data has been obtained are listed in the legend. WG4 is the data contained in Table 2 of [8] and shown for comparison purposes. The red full line shows the fitting function $D(T_{90})$, and the dashed lines envelop the range $D(T_{90}) \pm u_{\mathrm{combined}}(D(T_{90}))$, with the combined standard uncertainty $u_{\mathrm{combined}}(D(T_{90}))$. Right: The same as on the left but in a restricted temperature range.

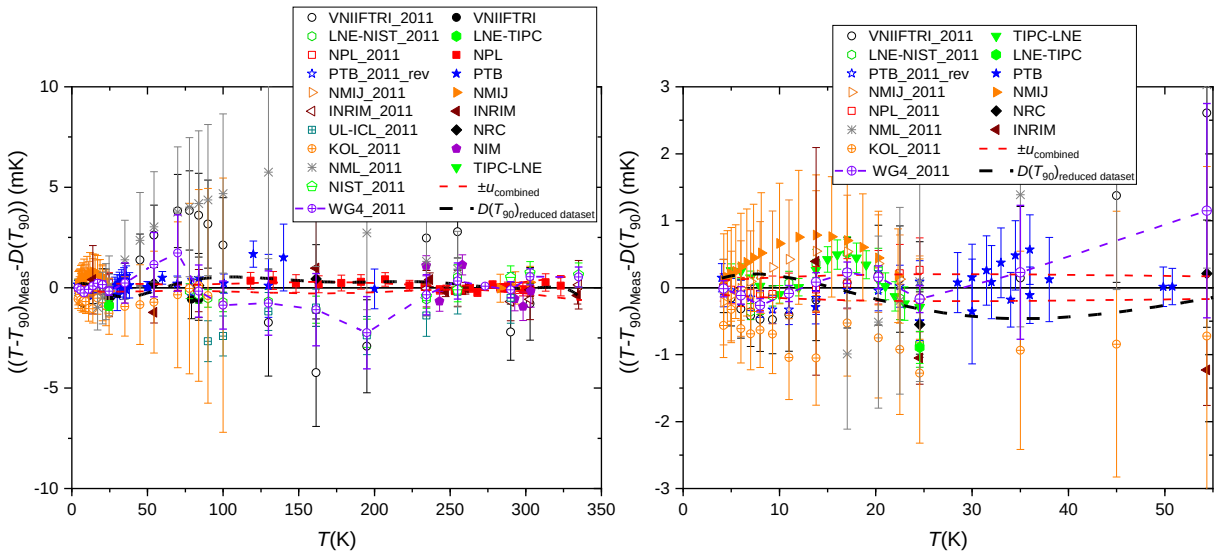

Figure 5: Left: The residual deviation of the $(T\text{-}T_{90})_{\mathrm{meas}}$ data listed in Tables 1 and 2 from the 12th order fit function $D(T_{90})$ is shown versus temperature. WG4 is the data contained in Table 2 of [8] and shown for comparison purposes. The red dashed lines envelop the range $\pm\, u_{\mathrm{combined}}(D(T_{90}))$, with the combined standard uncertainty $u_{\mathrm{combined}}(D(T_{90}))$. Right: The same as on the left but in a restricted temperature range.

4. Uncertainties

Table 3

The two dashed lines in Figure 5 plot the envelope of the standard uncertainty, $u(D(T_{90}))$, derived from three contributions. The first contribution, $u_{\mathrm{fit}}(D(T_{90}))$, is propagated from the uncertainties reported in the data used in the least squares fit (Tables 1 and 2). See [44] for the uncertainty propagation equations. The uncertainty propagation for weighted least-squares fits assumes the weighted residuals in the fit are independent and identically distributed. As Figure 2 shows, the residuals are very close to expectations. However, the patterns of residuals in Figure 5 shows the residuals are not independent. Correlations in the residuals arise from small systematic effects within each dataset, including non-uniqueness in the realisations of ITS-90 used in each experiment. To investigate the effects of correlations, generalised least-squares fits with non-diagonal covariance matrices were performed. It was found that the fit uncertainties were insensitive to modest correlations and unreasonably large correlations were required to yield any significant effects. Therefore, the effects of correlations are assumed to be negligible.

The second contribution to the uncertainty, $u(T - T_{90})_{\mathrm{TPW}}$, arises from the fact that most of the measurements of $(T - T_{90})$ used the TPW as a reference, and the uncertainty in the thermodynamic temperature of the TPW, $u(T_{\mathrm{TPW}})$, is now 0.10 mK. Consequently, this uncertainty must be propagated to other temperatures by multiplying $u(T_{\mathrm{TPW}})$ with the ratio T/T_{TPW} and adding in quadrature to the fit uncertainty. Note that the best estimate of the thermodynamic temperature of the triple point of water remains 273.1600(1) K, and readers who wish to use the triple point of water as a thermodynamic reference point should continue to use this value and uncertainty.

The third contribution is the non-uniqueness of the ITS-90, $u(T_{90})_{\mathrm{NU}}$. It consists of different sub contributions. In the present work, the dominating one is by nature a component that cannot be reduced. It is an inherent feature of the ITS-90 itself and not of the individual standard platinum resistance thermometer as interpolation instrument. The complete input from Table 2 and partially the input from Table 1 already includes the non-uniqueness component. For the present $(T - T_{90})$ data this component is a clear and omnipresent Type B component and cannot be reduced by averaging of different results as in this case for a fit to different data sets.

It is clearly visible in Table 4, that for temperatures below 25 K and above 255 K, the uncertainty of the fit $u_{\mathrm{fit}}(D(T_{90}))$ is below $u(T_{90})_{\mathrm{NU}}$. Consequently, to avoid underestimation of the overall uncertainty, it is preferable to allow for a potential double counting in some cases because the size of a possible overestimation is acceptable. Below 25 K, the estimates for the non-uniqueness are based on the standard deviation of the results obtained in Key Comparisons CCT-K1 [49] and EURAMET.T-K1.1 [50] in the temperature range from 4K to 25K. From 25 K to 335 K, recommendations of the CCT were considered that are given in [51].

The combination of the uncertainty components leads finally to the combined standard uncertainty $u(D(T_{90}))$ shown by the dashed lines in Figure 5. Numerical values of the uncertainty are tabulated in Table 4 at the same temperatures as treated in [8]. A polynomial of 6th order has also been fitted to the uncertainty estimates listed in Table 4 to give a simple smooth functional description. The coefficients are also listed in Table 3.

The uncertainty $u(D(T_{90}))$ is the uncertainty in the correction $D(T_{90})$. To obtain the uncertainty in the thermodynamic temperature, this uncertainty must be added in quadrature to the uncertainty in users' realisations of ITS-90. Guidance on the realisation of ITS-90 and on the calculation of the uncertainty can be found in the online BIPM guides [52].

The function $D(T_{90})$ is valid in the range of the fitted data from 4 K to 335 K, with a reduction in uncertainty of an order of magnitude compared to those given in [8]. Users working in a broader temperature range above and below 335 K might be interested in a smooth correction. A smooth transition from the new function $D(T_{90})$ to the old WG4 fitting function for temperatures from the TPW up to the copper point, $D_{2011}(T_{90})$, deduced in [8], is the point of intersection at T_{90} = 288.418 K. $D_{2011}(T_{90})$ is given by

$$D_{2011}(T_{90})\,/\,\mathrm{mK} = (T - T_{90})\,/\,\mathrm{mK} = (T_{90}\,/\,\mathrm{K})\sum_{i=0}^{4} c_i\,(273.16\,\mathrm{K}\,/\,T_{90})^{2i}\,, \qquad (7)$$

with c_0 = 0.0497; c_1 = -0.3032; c_2 = 1.0254; c_3 = -1.2895 and c_4 = 0.5176 (for more details see [8]). In addition, the change of slope at the transition point is very small. If the user is only interested in the temperature range below 335 K, the new function $D(T_{90})$ is recommended.

Table 4

5. Summary and conclusions

Since 2011, when the previous estimates of $(T - T_{90})$ were published by the CCT, there has been a change in the definition of the kelvin, and significant advances in primary thermometry were achieved, yielding much improved measurements of $(T - T_{90})$ over the range from 4 K to 323 K.

The analysis here combines the new data with the older data used in the 2011 analysis to update the consensus values for ($T - T_{90}$) over the range from 4K to 323 K. The updated values are represented by a 12th-order polynomial (coefficients listed in Table 3) with uncertainties given by a 6th-order polynomial (Table 3). The uncertainties in the ($T - T_{90}$) values are now comparable with the uncertainty in the best primary measurements of thermodynamic temperatures and the uncertainties in ITS-90 realisations. So, in combination with ITS-90 measurements, the results presented here offer an important means for achieving a state-of-the-art determination of thermodynamic temperature without the high cost and inconvenience of primary thermometry.

For the temperature range below 4 K, the recommendations of [8] should be used. From 0.65 K to 2 K, the application of the helium-3 vapour-pressure scale PTB-2006 [53] is recommended. This scale is consistent with the Provisional Low Temperature Scale of 2000, PLTS-2000 [54], from 0.65 K to 1 K. From 2 K to 4 K, the ITS-90 can be used. In this range, PTB-2006 and ITS-90 are equivalent. The recommendation is supported by a recently performed direct comparison of the melting and vapour pressures of helium-3 at the LNE [55]. The overview [56] shows that the thermodynamic deviation of the ITS-90 below 1.5 K has been verified consistently in three different ways by two independent groups in each case.

Acknowledgement

The authors thank Peter Saunders for sharing the non-linear least-squares fit software used for the fit and the estimation of the fit uncertainty. For some authors parts of their work was performed in the framework of the project 18SIB02 Real-K which has received funding from the EMPIR programme co-financed by the Participating States and from the European Union's Horizon 2020 Research and Innovation programme.

References

[1] Stock M. *et al*. 2019 *Metrologia* **56**, 022001

[2] Göbel E. O. and Siegner U. 2019 "The New International System of Units (SI)" (Wiley-VCH, Berlin) ISBN 978-3-527-34459-8

[3] White D. R. 2020 *Contemporary Physics*, **61**, 256

[4] https://ww w.bipm.org/en/publications/mises-en-pratique

[5] Fellmuth B. *et al.* 2016 *Phil. Trans. R. Soc.* A **374**, 20150037

[6] Preston-Thomas H. 1990 *Metrologia* **27**, 3 and 107

[7] Fellmuth 2018 *Guide to the Realization of the ITS-90, Part 1 – Introduction* https://www.bipm.org/en/committees/cc/cct/guides-to-thermometry

[8] Fischer J. *et al.* 2011 *Int. J. Thermophys.* **32**, 12

[9] https://www.bipm.org/en/committees/cc/cct/temperature-scales

[10] Fellmuth B. *et al.* 2006 *Meas. Sci. Technol.* **17**, R145

[11] Fischer J. *et al.* 2018 *Metrologia* **55**, R1

[12] JCGM 100:2008: Evaluation of measurement data — Guide to the expression of uncertainty in measurement

[13] Benedetto G. *et al.*, 2004 *Metrologia* **41**, 74

[14] Pitre L. *et al.*, 2006 *Metrologia* **43**, 142

[15] Moldover M.R. *et al* 1999 *J. Res. Natl. Inst. Stand. Technol.***104**, 11

[16] Ripple D.C. *et al* 2007, *Int. J. Thermophys.* **28**, 1789

[17] Strouse G.F. *et al* 2003, in *Temperature: Its Measurement and Control in Science and Industry*, vol. 7, ed. by D.C. Ripple (AIP, Melville, New York, 2003), 31

[18] Ewing M.R. and Trusler J.P.M, 2000 *J. Chem. Thermodyn.* **32**, 1229

[19] Luther H. *et al* 1996, *Metrologia* **33**, 341

[20] Gaiser et al., 2008 *Int. J. Thermophys.* **29**, 18

[21] Gaiser C. *et al.* 2017 *Metrologia* **54**, 141

[22] Astrov D.N. *et al.*, 1995 *Metrologia* **32**, 393

[23] Steur P.P.M. and Durieux M., 1986 *Metrologia* **23**, 1

[24] Tamura O. *et al.*, 2008, *Int. J. Thermophys.* **29**, 31

[25] Kemp R.C., *et al.*, 1986 *Metrologia* **23**, 61

[26] Berry K.H., 1979 *Metrologia* **15**, 89

[27] Gavioso R.M. *et al.* 2019 *Metrologia* **56**, 045006

[28] Zhang K. *et al.* 2020 *Metrologia* **57**, 024004

[29] Underwood R. *et al.* 2017 *Int. J. Thermophys*. **38**: 44

[30] Kytin V.G. *et al.* 2020 *Int. J. Thermophys.* **41**: 88

[31] Pan. C. *et al.* 2021 *Metrologia* **58**, 045006

[32] Widiatmo J. V. et al., 2020 *Int. J. Thermophys.* **41**:42

[33] Gaiser C. *et al.* 2020 *Metrologia* **57**, 055003

[34] Gaiser C. and Fellmuth B. 2021 *Metrologia* **58**, 042101

[35] Rourke P.M.C. 2020 *Metrologia* **57**, 024001

[36] Madonna Ripa D. *et al.* 2021 *Metrologia* **58**, 069501

[37] Gao B. *et al.* 2021 *Metrologia* **58** 059501

[38] Nakano T. *et al.* 2017 *Int. J. Thermophys.* **38**:105

[39] Mohr P.J. *et al.* 2018 *Metrologia* **55**, 125

[40] Björck Å. 1967 *BIT Numerical Mathematics* **7**, 1

[41] Björck, Å. 1996, Numerical methods for least squares problems. *Society for Industrial and Applied Mathematics*

[42] Saunders P. 2016 *Callaghan Innovation Report* **18** (5.3)

[43] Saunders P. 2003 *Metrologia* **40**, 93

[44] Press, W. H. *et al.* 2007, Numerical recipes 3rd edition: The art of scientific computing. (Cambridge University Press), 3rd edition

[45] Powell R.L. *et al*. 1972 *Temperature, its Measurement and Control in Science and Industry*, edited by H. H. Plumb (Inst. Soc. of America, Pittsburgh, 1972) **4**, 1423

[46] Burnham, K. P. and Anderson D. R. 2004 *Sociological Methods & Research.* 33.2, 261

[47] Rusby, R. L. 2010 *Int. J. Thermophys.* **31,** 1567

[48] Crovini L. *et al* 1991 *Metrologia* **28**, 317

[49] Rusby R.L. *et al.* 2006 *Metrologia* **43**, 03002

[50] Gaiser C. *et al.* 2017 *Metrologia* **54**, 03002

[51] Pokhodun *et al.* 2018 Guide to the realization of the ITS-90: Chapter 5: Platinum Resistance Thermometry, Edition 2018. CCT publications: Guidance documents: http://www.bipm.org/utils/common/pdf/ITS-90/Guide_ITS-90_5_SPRT_2018.pdf

[52] https://www.bipm.org/en/committees/cc/cct/guides-to-thermometry

[53] Engert J. *et al.* 2007 *Metrologia* **44**, 40

[54] Rusby R.L. *et al.* 2002 *J. low temp. phys*. **126**, 633

[55] Pan. C. *et al.* 2021 *Metrologia* **58**, 025005

[56] Fellmuth B. *et al.* 2023 *Metrologia*, to be submitted

Table 1: $\Delta = (T - T_{90})$ input data together with uncertainty estimates. The references are given in the top row. The uncertainty values marked with an asterisk are the ones used for estimating of $U_{\mathrm{minexp}\,(k=1)}$ shown in Figure 3. Dataset PTB_2011_org is superseded by PTB_2011_rev. It is listed to allow for complete reproduction of the values published in [8] see footnote [1].

	VNIIFTRI_2011 [22]		INRIM_2011 [13]		NPL_2011 [29]		PTB_2011_org [19,20]		PTB_2011_rev [21]		UL-ICL_2011 [18]		NML_2011 [25]		KOL_2011 based on [23]		NIST_2011 [15-17]),		LNE_NIST_2011 [14]		NMIJ_2011 [24]	
T_{90}	Δ	u_Δ	Δ	u_Δ	Δ	u_Δ	Δ	u_Δ	Δ	u_Δ	Δ	u_Δ	Δ	u_Δ	Δ	u_Δ	Δ	u_Δ	Δ	u_Δ	Δ	u_Δ
4.2	0.02	0.40			0.00	0.20	0.04	0.17	-0.07	0.23					-0.57	0.48					-0.22	0.64
5	-0.08	0.42			0.04	0.21	0.24	0.18	0.03	0.18					-0.25	0.50					-0.05	0.67
6	-0.16	0.44			0.09	0.22	0.10	0.19	0.09	0.19					-0.46	0.52					0.14	0.71
7	-0.20	0.46			0.14	0.23	-0.03	0.2	0.07	0.19					-0.47	0.54			-0.14	0.12	0.31	0.76
8	-0.20	0.48			0.18	0.25	-0.04	0.2	0.03	0.20					-0.36	0.56			0.01	0.13	0.46	0.80
9.288	-0.16	0.51			0.23	0.27	0.04	0.22	-0.01	0.21					-0.37	0.59			0.20	0.15	0.62	0.84
11	-0.05	0.54			0.28	0.30	0.14	0.23	0.03	0.22					-0.69	0.63			0.43	0.17	0.78	0.89
13.8033	0.17	0.61			0.33	0.34	0.26	0.25	0.20	0.24					-0.70	0.70			0.72	0.21	0.90	0.91
17.035	0.36	0.68			0.35	0.37	0.41	0.28	0.25	0.27			-0.70	1.12	-0.24	0.80			0.80	0.25	0.83	0.84
20.27	0.35	0.75			0.32	0.40	0.28	0.31	0.12	0.30			-0.35	1.29	-0.59	0.90			0.46	0.29	0.52	0.73
22.5	0.18	0.80			0.27	0.43	0.31	0.33	0.08	0.31			-0.14	1.40	-0.87	0.97			-0.10	0.32	0.18	0.66
24.5561	-0.21	0.84			0.21	0.48	0.42	0.35	0.03	0.31			0.03	1.49	-1.34	1.05			-0.90	0.35	-0.23	0.64
35	-0.62	1.07											0.63	1.97	-1.70	1.48						
45	-0.14	1.29											0.85	2.39	-2.35	1.98						
54.3584	0.40	1.50											0.82	2.74	-2.93	2.54						
70	0.52	1.82											0.46	3.25	-3.66	3.63						
77.657	0.04	1.97											0.20	3.47	-3.84	4.24			-3.98	0.37*		
83.8058	-0.60	2.09											-0.02	3.62	-4.10	4.77			-4.58	0.40*		
90	-1.46	2.19									-7.29	1.02	-0.26	3.76	-5.03	5.34			-5.16	0.44*		
100	-3.20	2.35									-7.74	1.00	-0.64	3.96	-6.19	6.33			-6.04	0.48		
130	-9.04	2.67									-8.49	0.94	-1.55	4.31					-7.98	0.60		
161.405	-11.57	2.68									-8.33	0.93	-2.00	4.29					-8.44	0.68		
195	-7.65	2.32									-7.11	0.95	-2.00	3.83					-7.00	0.70		
234.3156	-0.42	1.61	-2.95	0.91							-4.28	1.04	-1.59	2.72			-3.33	0.60	-3.48	0.67		
255	0.81	1.30	-2.01	0.90							-2.18	1.11	-1.05	1.88			-2.08	0.60	-1.45	0.62		
273.16	In 2011, T-T_{90}=0 mK with $u(T$-$T_{90})$=0; after the redefinition of the kelvin, still T-T_{90}=0 mK, but now $u(T$-$T_{90})$=0.10 mK temperature equivalent uncertainty of the Boltzmann constant right before its redefinition)."																					
290	0.08	1.40	1.61	0.96							1.78	1.26					2.81	0.56				
302.9146	3.04	1.87	3.26	1.01													4.58	0.57				
335			7.23	1.21													7.72	0.60				

Table 2: $\Delta = (T - T_{90})$ input data together with uncertainty estimates. The references are given in the top row. The data points highlighted in red are the ones used for the reduced dataset (see Figure 3). The uncertainty values marked with an asterisk are the ones used for estimating $U_{\mathrm{minexp}\,(k=1)}$ shown in Figure 3

TIPC-LNE [36]			LNE-TIPC [30]			INRIM [27, 36]			NIM [28]			NMIJ [32, 38]			NPL [29]			NRC [35]			PTB [21, 33, 34]			VNIIFTRI [30]		
T_{90}	Δ	u_Δ	T_{90}	Δ	u_Δ	T_{90}	Δ	u_Δ	T_{90}	Δ	u_Δ	T_{90}	Δ	u_Δ	T_{90}	Δ	u_Δ	T_{90}	Δ	u_Δ	T_{90}	Δ	u_Δ	T_{90}	Δ	u_Δ
24.55535	-0.35	0.26	24.5561	-0.95	0.24*	13.8033	0.75	1.7	234.2107	-1.8	0.5	4.22194	0.10	0.7	118.15	-6.27	0.42	24.5561	-0.61	0.49	28.5	-0.23	0.45	83.8058	-4.81	1.02
23.00025	-0.21	0.25				24.5561	-1.11	0.39	243.1051	-3.3	0.5	4.59018	0.19	0.7	133.15	-7.08	0.44*	54.3584	-2	0.8	30	-0.25	0.50	79	-4.47	0.97
21.99973	-0.05	0.22*				54.3584	-3.44	0.53	258.078	-0.6	0.5	5.00227	0.27	0.7	148.15	-7.5	0.44	83.8058	-4.1	1.6	30	-0.76	0.78			
20.99828	0.15	0.2				83.8058	-4.35	1.05	292.6937	2.1	0.6	5.47085	0.35	0.7	163.15	-7.08	0.42*	161.406	-6.9	1.7	31.5	-0.25	0.52			
20.2679	0.28	0.19*				161.406	-6.37	2.9	298.2272	2.4	0.7	6.00147	0.47	0.8	178.15	-5.94	0.39				32	-0.46	0.55			
18.99873	0.56	0.21				236.619	-2.43	0.34	303.2614	3.7	0.8	6.59957	0.57	0.8	191.15	-4.76	0.36*				33	-0.24	0.52			
17.99977	0.7	0.22*				247	-2.65	0.25				7.30268	0.68	0.8	207.15	-3.46	0.34				34	-0.87	0.41*			
17.03389	0.79	0.22				260.12	-1.58	0.29				8.1035	0.80	0.9	223.15	-3.08	0.26				34.5	-0.24	0.52			
16.00012	0.81	0.22				302.9146	3.73	0.33				10.001	1.00	0.9	233.15	-2.83	0.23*				36	-0.95	0.42			
15.00062	0.76	0.19				334.17	6.57	0.42*				12.0011	1.12	1	243.15	-2.73	0.21				36	-0.26	0.52			
13.80428	0.62	0.16*										13.8044	1.14	0.9	253.15	-2.26	0.19*				38	-0.86	0.63			
12.00052	0.37	0.13*										15.4197	1.09	0.9	258.15	-1.86	0.21				130	-7.21	1.57			
10.00094	0.24	0.13*										17.036	0.99	0.9	263.15	-1.29	0.2				140	-6.15	1.67			
8.00097	0.3	0.11*										18.6461	0.83	0.8	268.15	-0.94	0.2				49.83501	-1.86	0.30*			
7.00026	0.37	0.1*										20.2706	0.61	0.7	278.15	0.77	0.18				50.786863	-1.93	0.27			
6.00006	0.4	0.11*										22.3002	0.25	0.7	283.15	1.32	0.21				59.784505	-2.11	0.31*			
5.00021	0.33	0.1*										24.5559	-0.23	0.6	288.15	2.06	0.25*				69.738738	-3.09	0.39*			
												283.15	1.3	0.7	293.15	2.70	0.28				78.558011	-3.82	0.42			
												293.15	2.7	0.8	298.15	3.24	0.32				100.49553	-5.16	0.48*			
												302.9146	4.1	0.8	303.15	3.79	0.32*				200.08784	-4.40	0.99			
															313.15	5.00	0.43				84	-3.74	0.43			
															323.15	5.68	0.51				120	-5.06	0.65			
																					3.99831	0.12	0.21*			
																					13.76466	0.07	0.25			
																					24.55518	-0.56	0.28			

Table 3: Fitting coefficients for the power series approximating the T -T_{90} input data **(**$D(T_{90})$: α_i) and its standard uncertainty estimates ($u_{\text{combined-LS}}(D(T_{90}))$: β_i) resulting from a least squares (LS) fit to u_{combined} in specific temperature ranges, respectively.

i	α_i	β_i
0	-6.393509785E-01	6.362639E-02
1	2.044362025E-01	1.251359E-02
2	-1.453482491E-02	-3.880108E-04
3	4.860355653E-04	4.878407E-06
4	-1.152913045E-05	-2.789077E-08
5	1.932372065E-07	7.268939E-11
6	-2.222708123E-09	-6.999818E-14
7	1.722390583E-11	
8	-8.878574513E-14	
9	2.985516966E-16	
10	-6.273436285E-19	
11	7.467125710E-22	
12	-3.840581614E-25	

Table 4: The fitting function ($T - T_{90}$) versus T_{90}, $D(T_{90})$, is tabulated at the same temperatures as in [8]. In the next column the uncertainty of the weighted fit $u_{\mathrm{fit}}(D(T_{90}))$ is listed. The following columns give the contributions that must be added to $u_{\mathrm{fit}}(D(T_{90}))$ to give finally $u(D(T_{90}))$ as a combined uncertainty estimate for $D(T_{90})$. The $u_{\mathrm{combined}}(D(T_{90}))$ values can be accessed in fitted form by the power series of 6th order ($u_{\mathrm{combined\text{-}LS}}(D(T_{90}))$) using the coefficients β_i given in Table 3.

T/K	$D(T_{90})$ / mK	$u_{\mathrm{fit}}(D(T_{90}))$ / mK	$u(T - T_{90})_{\mathrm{TPW}}$ / mK	$u(T_{90})_{\mathrm{NU}}$ / mK	$u_{\mathrm{combined}}(D(T_{90}))$ / mK
4.2	0.00	0.06	0.00	0.12	0.13
5	0.07	0.05	0.00	0.12	0.13
6	0.16	0.03	0.00	0.12	0.12
7	0.22	0.03	0.00	0.12	0.12
8	0.27	0.03	0.00	0.12	0.13
9.288	0.32	0.04	0.00	0.12	0.13
11	0.36	0.04	0.00	0.14	0.15
13.8033	0.36	0.04	0.01	0.19	0.19
17.035	0.29	0.04	0.01	0.19	0.19
20.27	0.16	0.05	0.01	0.19	0.19
22.5	0.05	0.05	0.01	0.19	0.19
24.5561	-0.06	0.06	0.01	0.19	0.20
35	-0.76	0.10	0.01	0.24	0.26
45	-1.51	0.13	0.02	0.11	0.17
54.3584	-2.21	0.14	0.02	0.00	0.14
70	-3.30	0.14	0.03	0.07	0.15
77.657	-3.80	0.14	0.03	0.05	0.15
83.8058	-4.21	0.15	0.03	0.00	0.15
90	-4.62	0.15	0.03	0.05	0.16
100	-5.32	0.17	0.04	0.10	0.20
130	-7.30	0.21	0.05	0.16	0.27
161.405	-7.34	0.21	0.06	0.16	0.27
195	-4.73	0.18	0.07	0.12	0.23
234.3156	-2.89	0.10	0.09	0.00	0.13
255	-1.97	0.08	0.09	0.09	0.15
273.16	-0.07	0.07	0.10	0.00	0.12
290	2.29	0.09	0.11	0.18	0.23
302.9146	3.84	0.14	0.11	0.28	0.34
335	7.09	0.37	0.12	0.46	0.60